

# Structure of a Sliding Clamp on DNA

Roxana E. Georgescu,<sup>1</sup> Seung-Sup Kim,<sup>2</sup> Olga Yurieva,<sup>1</sup> John Kuriyan,<sup>3,4,5,6</sup> Xiang-Peng Kong,<sup>2</sup> and Mike O'Donnell<sup>1,\*</sup>

<sup>1</sup>Howard Hughes Medical Institute, Rockefeller University, 1230 York Avenue, Box 228, New York, NY 10021, USA

<sup>2</sup>Department of Biochemistry, NYU School of Medicine, 550 First Avenue, New York, NY 10016, USA

<sup>3</sup>Howard Hughes Medical Institute

<sup>4</sup>Department of Molecular and Cellular Biology

<sup>5</sup>Department of Chemistry

University of California, Berkeley, 401 Barker MC 3202, Berkeley, CA 94720, USA

<sup>6</sup>Physical Biosciences Division, Lawrence Berkeley National Lab, Berkeley, CA 94720, USA

\*Correspondence: [odonnell@mail.rockefeller.edu](mailto:odonnell@mail.rockefeller.edu)

DOI 10.1016/j.cell.2007.11.045

## SUMMARY

The structure of the *E. coli*  $\beta$  clamp polymerase processivity factor has been solved in complex with primed DNA. Interestingly, the clamp directly binds the DNA duplex and also forms a crystal contact with the ssDNA template strand, which binds into the protein-binding pocket of the clamp. We demonstrate that these clamp-DNA interactions function in clamp loading, perhaps by inducing the ring to close around DNA. Clamp binding to template ssDNA may also serve to hold the clamp at a primed site after loading or during switching of multiple factors on the clamp. Remarkably, the DNA is highly tilted as it passes through the  $\beta$  ring. The pronounced 22° angle of DNA through  $\beta$  may enable DNA to switch between multiple factors bound to a single clamp simply by alternating from one protomer of the ring to the other.

## INTRODUCTION

Chromosomal replicases achieve highly processive DNA synthesis through attachment to a ring-shaped sliding clamp processivity factor (reviewed in Johnson and O'Donnell, 2005; McHenry, 2003). Sliding clamps in all three domains of life require a multiprotein clamp loader that assembles the clamp onto DNA. The bacterial  $\beta$  clamp is a homodimer; each monomer consists of three globular domains to yield a six-domain ring (Argiriadi et al., 2006; Kong et al., 1992). The eukaryotic sliding clamp proliferating cell nuclear antigen (PCNA) is also a six-domain ring with similar dimensions and chain-fold to bacterial  $\beta$ , except PCNA is a homotrimer and therefore each monomer consists of only two domains (Gulbis et al., 1996; Krishna et al., 1994). The protomers of both  $\beta$  and PCNA are arranged head to tail, which results in structurally distinct surfaces on the two "faces" of the clamps. The C termini protrude from one face, sometimes referred to as the C-terminal face, and the N termini from the other. Both  $\beta$  and PCNA contain a hydrophobic pocket on the surface of the C-terminal face to which the polymerase and clamp loader attach.

Although  $\beta$  and PCNA were originally identified as processivity factors for their respective chromosomal DNA polymerases, it is

now clear that many proteins bind to sliding clamps. For example, all five *E. coli* DNA polymerases bind the  $\beta$  clamp, as do DNA ligase, MutS, MutL, and the Hda cell-cycle regulatory factor (reviewed in Johnson and O'Donnell, 2005). Eukaryotic PCNA also interacts with diverse DNA polymerases and many other proteins involved in DNA repair and cell-cycle control (Warbrick, 2000). Clamp-binding proteins all appear to bind the hydrophobic protein-binding pocket on the C-terminal face of the clamp, although they likely have unique touch points as well (Bunting et al., 2003; Chapados et al., 2004; Gulbis et al., 1996; Jeruzalmi et al., 2001; Matsumiya et al., 2001; Shamoo and Steitz, 1999; Sutton and Walker, 2001; Sutton and Duzen, 2006). Proteins that bind PCNA and  $\beta$  typically do so via a conserved sequence (Dalrymple et al., 2001; Warbrick, 2000), and the homooligomeric structure of  $\beta$  and PCNA may provide the ability to bind more than one protein at the same time. Mechanisms by which multiple proteins coordinate action on sliding clamps is a topic of active investigation (Fujii and Fuchs, 2004; Goodman, 2002; Indiani et al., 2005; Sutton, 2004; Sutton and Walker, 2001).

DNA is generally modeled straight through  $\beta$  and PCNA, perpendicular to the plane of the ring. Interestingly, recent molecular simulations of PCNA suggest that DNA may adopt a tilt of up to 20° through the ring (Ivanov et al., 2006). However, a sliding clamp bound to DNA has not been directly observed, and therefore we set out to obtain a cocrystal of the *E. coli*  $\beta$  clamp bound to DNA. We were surprised to find in biochemical studies reported here that  $\beta$  binds DNA specifically and interacts with both double-strand (ds) DNA and single-strand (ss) DNA. These findings encouraged us to use small linear DNAs in attempts to crystallize the  $\beta$ -DNA complex. Conditions that lead to cocrystals of  $\beta$  bound to DNA were developed by devising a rapid visual screen for cocrystals that utilize DNA molecules labeled with a chromophore.

The cocrystal structure presented herein consists of  $\beta$  in complex with a primed DNA site. The structure reveals several interesting  $\beta$ -DNA contacts, including residues on surface loops. The DNA passes through the ring at a steep 22° angle. Moreover, the template ssDNA of the primed site forms a crystal contact with the adjacent  $\beta$  where it binds the protein-binding pocket of the clamp. Studies of site-specific  $\beta$  mutants confirm that binding of  $\beta$  to both dsDNA and ssDNA plays key roles in the clamp loading mechanism.

The fact that the clamp recognizes primed DNA has implications for clamp loading and also suggests mechanisms by which

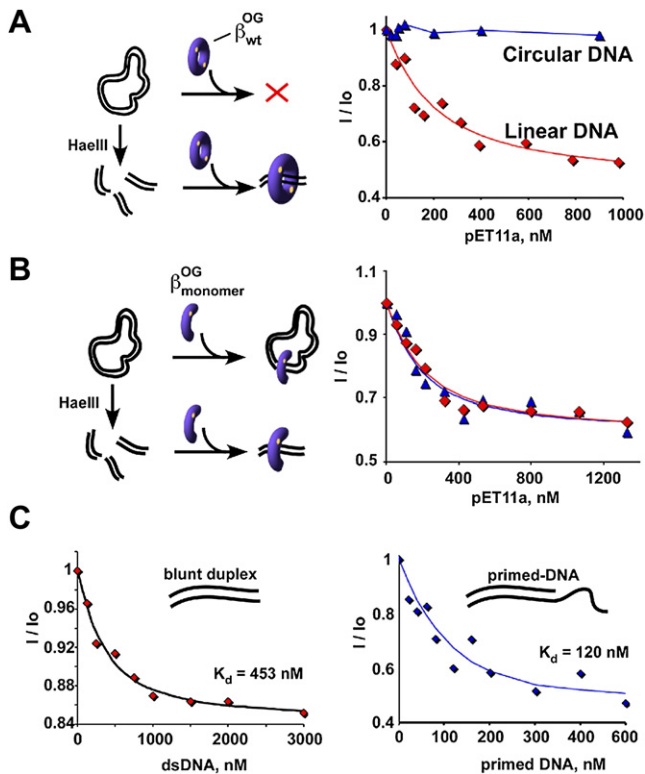


**Figure 1.  $\beta$  Binds DNA Independent of the Circular Shape of the Clamp**

(A) Either circular pET11a plasmid DNA (triangles) or linear DNA fragments (diamonds) produced by HaeIII digestion of the plasmid are titrated into a solution containing  $\beta^{\text{OG}}$ .

(B) The experiment of (A) was repeated with the  $\beta$  monomer mutant.

(C) Titration of an 18 bp duplex into  $\beta^{\text{OG}}$  (left). Titration of a primed template (18/28) into  $\beta^{\text{OG}}$  (right). Curve fitting (A+B  $\rightarrow$  AB) yields the apparent  $K_d$  values shown in each plot.

different proteins that bind the clamp may switch with one another on  $\beta$  and the DNA that it encircles.

## RESULTS

### Direct Interaction of $\beta$ with DNA

The  $\beta$  clamp binds DNA by encircling it and slides along the duplex. This topological binding mode conceptually precludes formation of ordered cocrystals of DNA bound to  $\beta$ . However, the experiments of Figure 1A indicate that  $\beta$  binds DNA directly, independent of its circular shape. In this experiment,  $\beta$  was labeled with a fluorophore ( $\beta^{\text{OG}}$ ), and then circular duplex pET11a plasmid, or HaeIII-digested pET11a, was titrated into  $\beta^{\text{OG}}$ . The results indicate that the linearized DNA binds  $\beta^{\text{OG}}$ , whereas circular DNA does not, consistent with the absence of a clamp loader in this assay. One may expect that  $\beta$  would bind linear DNA, because linear DNA can diffuse into the closed ring without need for a clamp loader. However, under the dilute conditions of these assays,  $\beta$  that binds linear DNA only by encircling it will rapidly slide back off the DNA, and the amount of  $\beta$ -DNA complex at equilibrium would be expected to be negligible. Yet the observed

binding curve indicates saturation and therefore complete  $\beta$ -DNA complex formation.

Complete formation of a  $\beta$  linear DNA complex suggests that  $\beta$  has direct contacts with DNA, regardless of its ring shape. To test whether binding of  $\beta$  to DNA is independent of the ring shape of the clamp, we repeated the assay with a  $\beta$  monomer mutant (Jeruzalmi et al., 2001). The result, in Figure 1B, shows that the  $\beta$  monomer mutant still binds linear DNA and, in fact, binds circular DNA too. Binding of both linear and circular DNA to the  $\beta$  monomer mutant supports the conclusion that  $\beta$  interacts with DNA directly, independent of its circular shape. Moreover, the fact that the wild-type (WT)  $\beta$  ring does not bind circular DNA suggests that DNA must access the central cavity of  $\beta$  to exhibit binding.

Next the DNA binding assay was used to quantitate the affinity between  $\beta$  and a short synthetic blunt DNA duplex. The result, in Figure 1C, yields an apparent  $K_d$  value of 453 nM. The experiment was then repeated with a short primed template, with the result that  $\beta$  binds a primed site about 4-fold tighter than the blunt duplex ( $K_d$  value, 120 nM; Figure 1C). This finding implies that  $\beta$  has binding sites for both dsDNA and ssDNA regions of a primed site, and this is confirmed in the crystal structure presented below.

### Visual Screen for Cocrystals

$\beta$  crystallizes easily by itself, and therefore we wished to develop a rapid screen for  $\beta$ -DNA cocrystals, ensuring the presence of DNA in the  $\beta$  crystal before taking it to a synchrotron. A simple and rapid screen for  $\beta$ -DNA cocrystals was provided by using DNA substrates tagged with a chromophore that allow rapid identification of cocrystals by simply inspecting for color. This made it possible to test a variety of conditions and different DNA substrates for cocrystal formation. In the current study, DNA was 5' end labeled with Cy5 (blue). DNA structures that vary in their lengths of duplex and ssDNA were examined for cocrystal formation with  $\beta$ . This method, which used a 10 bp duplex and 5' ssDNA extensions of various lengths, led to conditions that produced brightly colored blue crystals (Figure 2A). To rule out fortuitous binding of the Cy5 moiety to  $\beta$ , a series of 5'-TAMN-labeled DNAs were also tested. This time the resulting crystals were bright red (Figure 2A). Because the Cy5 and TAMN molecules have very different structures,  $\beta$  likely binds DNA and not the label.

The strategy of using chromophoric ligands to visually screen cocrystals should generalize to other DNA binding proteins. It should also apply to other types of ligands that can be labeled or are intrinsically chromophoric. Examples are shown in Figure S1, in which  $\beta$  is cocrystallized with a TAMN-labeled peptide corresponding to the C-terminal sequence in  $\alpha$  (DNA polymerase), which is known to bind  $\beta$  (Lopez de Saro et al., 2003). Figure S1 also shows colored cocrystals of the yeast PCNA clamp with DNA and of DNA cocrystals with  $\beta$  from a Gram-positive bacterium, *Streptococcus pyogenes*.

### Structure of the $\beta$ -DNA Complex

The structure of  $\beta$  bound to a 10/14-mer primed site was solved to 1.92 Å resolution by molecular replacement using native  $\beta$  (Kong et al., 1992) as the starting model (Table S1 available

online). Overall, the primer template is in reverse orientation, and possible reasons for this are described later. However, the duplex DNA is perfectly 2-fold symmetric and thus has no forward or reverse. We therefore initiate description of the structure with how the duplex portion of DNA goes through the  $\beta$  clamp, then discuss how template ssDNA binds to  $\beta$ .

The helical density of all 10 bp was immediately visible from the difference map (Figure 2B). The DNA is standard B form even though no restraints were placed during refinement on sugar pucker, torsion angles, or Watson-Crick hydrogen bonding. Analysis with the program 3DNA (Lu and Olson, 2003) shows an average helical twist of  $38.81^\circ$  and rise of  $\sim 3.26 \text{ \AA}$  per bp. Several residues contact DNA, illustrated in Figure 2C.

Interestingly, DNA is sharply tilted within the central channel, defining an angle of  $\sim 22^\circ$  from the C2 rotation axis of  $\beta$  (Figures 2B and 3A). The tilt allows dsDNA to make contacts with exposed R24 and Q149 (see Figures 3A and 3B), which lie on protruding loops on the C-terminal face of  $\beta$ , the face to which Pol III core and the clamp loader bind (Naktinis et al., 1996). The sharp tilt of DNA through  $\beta$  is consistent with recent PCNA-DNA modeling studies (Ivanov et al., 2006). Interaction with R24, Q149, and other  $\beta$ -DNA contacts (Figure 2C) likely defines the tilt, although a crystal contact to ssDNA (described later) may also contribute to the observed angle of DNA.

The inner surface of  $\beta$ , like processivity clamps of other organisms, is lined by  $\alpha$  helices that carry a net positive charge. Some of the basic side chains lining the inside channel of the  $\beta$  ring appear flexible (i.e., disordered, have high B factors, or exhibit different conformations in the two protomers) but become ordered in the cocrystal through contact with the phosphate backbone of DNA.

### R24 and Q149 Are Functional in Replication

Among the DNA-binding residues of  $\beta$ , highly conserved R24 and less-conserved Q149 lie on exposed surface loops of the C-terminal face of  $\beta$  to which proteins bind, suggesting they may be functional with other proteins. We therefore constructed alanine replacement mutants of R24 and Q149 and examined the  $\beta$  mutants in replication activity assays. In Figure 3C,  $\beta$  is titrated into reactions containing Pol III\* (a Pol III core-clamp loader complex) and primed M13 ssDNA coated with SSB. Activity in this assay requires both clamp loading and polymerase extension. The results show that the R24A/Q149A double mutant of  $\beta$  is greatly reduced in replication activity; the single mutants of  $\beta$  show intermediate defects. In the fluorometric assay for DNA binding (i.e., as in Figure 1), the  $\beta$  mutants show only  $\sim 2$ - to 3-fold defects, consistent with the presence of other residues (on the inside of  $\beta$ ) that interact with DNA (Figure 2C).

Mutation of R24 and Q149 may alter diffusion of  $\beta$  along DNA, creating a drag on the polymerase during chain extension. To test  $\beta$  mutants in chain extension speed, Pol III core was preincubated with large amounts of  $\beta$  (or  $\beta$  mutants) and singly primed M13 ssDNA along with only two dNTPs, giving time for the Pol III- $\beta$  complex to assemble on primed ssDNA (i.e., in case clamp loading is defective). Then synchronous chain extension was initiated by adding remaining dNTPs, and timed aliquots were analyzed in a native agarose gel. The product analysis demonstrates that the  $\beta$  mutants are as rapid as WT  $\beta$  in function with

Pol III core, and thus R24 and Q149 are not defective in elongation speed with Pol III (Figure 3D).

To address whether the  $\beta$  mutants are deficient in clamp loading, we designed a clamp loading assay using synthetic primed DNA immobilized to magnetic beads (see Figure 3E). Primed DNA is attached to beads via a 3' biotin-to-streptavidin linkage, and SSB is used to block clamps from sliding off. To monitor clamp loading,  $\beta$  is labeled with  $^{32}\text{P}$  via an N-terminal kinase tag, then clamp loading is initiated and quenched at the indicated times. The beads are collected by using a magnetic concentrator, and  $^{32}\text{P}$ - $\beta$  attached to the immobilized DNA is quantitated. The results demonstrate that the R24A/Q149 double mutant of  $\beta$  is highly deficient in clamp loading. The single amino acid mutants of  $\beta$  show intermediate levels of activity and are approximately equally defective in the clamp loading assay, which may be due to the high amount of  $\beta$  used in this assay or to other differences between the clamp loading and replication assays. The  $K_d$  of each  $\beta$  mutant for binding to the clamp loader is nearly the same as WT  $\beta$  (Figure S2), and thus the activity defect presumably lies in a central role for  $\beta$ -DNA interaction in the clamp loading mechanism itself (see Discussion).

It is interesting to note previous studies in which mutation of  $\beta$  residues 148–152 to Ala results in a noticeable defect with Pol III and a more severe defect with Pol IV (Sutton et al., 2005). Hence, Q149, eliminated in the  $\beta$ 148–152 mutant, is not essential, and perhaps the deficiency with Pol III may occur through its defect in clamp loading rate, whereas the greater defect with Pol IV may be due to loss of a direct contact between Pol IV and a mutated residue(s) on  $\beta$ .

### ssDNA Binds to the Protein-Binding Pocket of $\beta$

The ssDNA template of the primed DNA is visible in the electron density, and it forms a crystal contact with an adjacent molecule of  $\beta$  in the crystal lattice (see Figure 4A and Figure S4). The fact that the  $\beta$ -ssDNA interaction is a crystal contact (i.e., it is intermolecular) raises the question of whether it is simply a crystal artifact or has physiological significance. However, the contact is in a very interesting place; ssDNA enters the protein-binding site of the adjacent  $\beta$  clamp. The reason the ssDNA binds an adjacent clamp (i.e., forms a crystal contact) is because the primed DNA goes through  $\beta$  in reverse of normal. We believe the reason that the primed site is in reverse orientation in the crystal relative to the physiological orientation provided by the clamp loader is that the intermolecular  $\beta$ -ssDNA crystal contact promotes growth of the crystal lattice and that  $\beta$  is “blind” to the orientation of dsDNA, because the duplex is perfectly 2-fold symmetric.

The clamp loader ensures that  $\beta$  is correctly oriented on DNA, such that the primed/ssDNA junction extrudes from the C-terminal face containing the protein-binding pockets (as illustrated in Figures 6 and 7). We present three lines of experimental evidence that  $\beta$  binds primed DNA in the correct orientation when it is in solution. One line of evidence has already been presented:  $\beta$  binds primed DNA tighter than dsDNA in dilute solution (Figure 1), implying that both the ssDNA and dsDNA interact with  $\beta$ . The second line of evidence requires a closer look at the  $\beta$ -ssDNA interaction. ssDNA binds in a region on the surface of  $\beta$  that is lined with basic residues (Figure 4B). This region also contains two adjacent tyrosines (Y153 and Y154; see



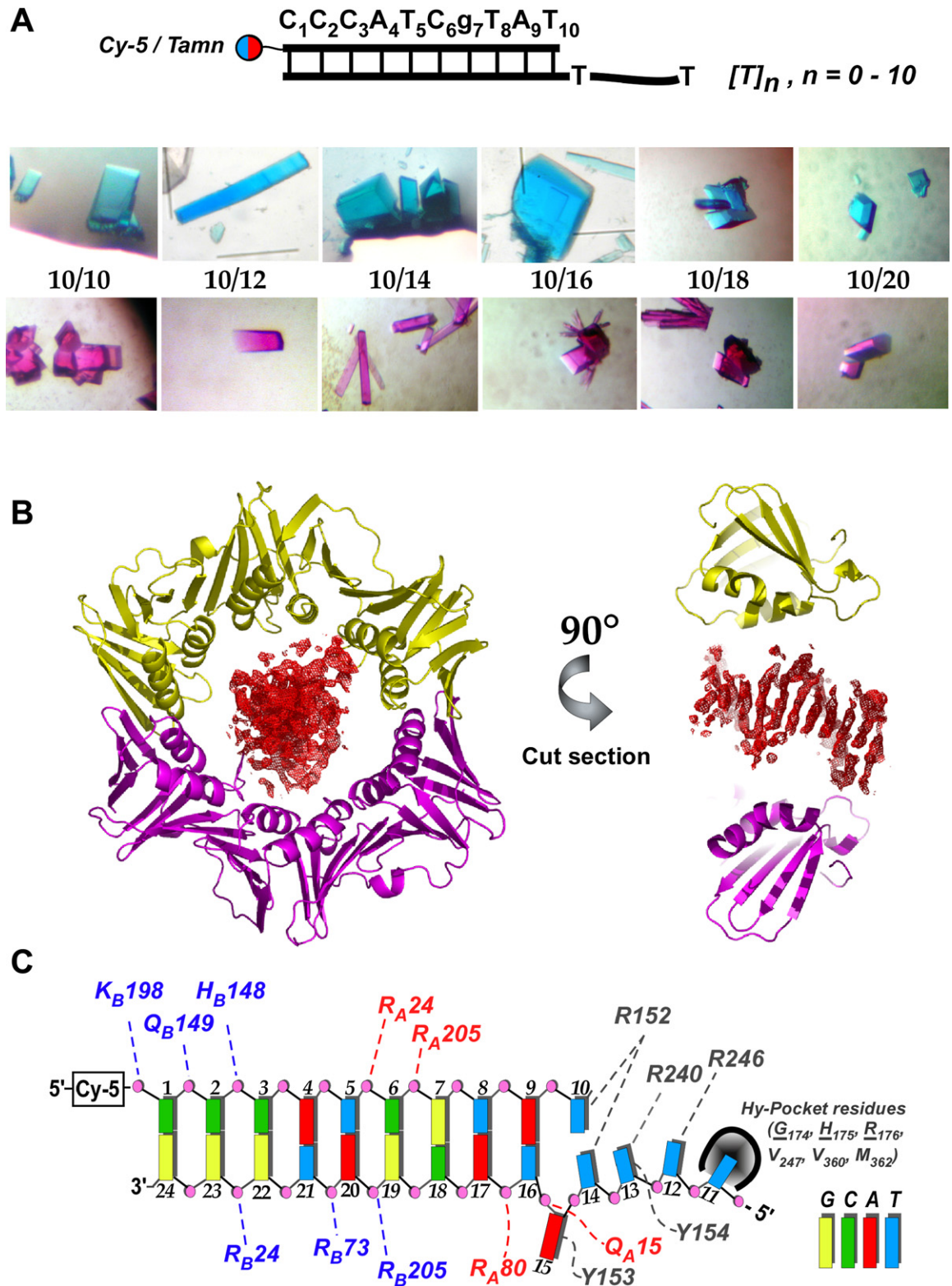


**Figure 2. Cocystal Color Screen and Electron Density of DNA in the  $\beta$ -DNA Complex**

(A) Cocystals of *E. coli*  $\beta$  with primed templates labeled at the 5' terminus with either Cy5- (top row) or TAMN- (bottom row).

(B) Electron density map of DNA in the interior of  $\beta$ : front and side views. Fourier difference maps with  $(F_o - F_c)$  coefficients in red contoured at 1.6  $\sigma$ .

Figure 4C) that stack with nucleotide bases (T13 and A15) that guide the ssDNA bases T11 and T12 into the protein-binding pocket, placing them next to conserved residues V247 (3.6 Å) and M362 (3.09 Å), and T11 may form an H bond to T172 (2.95 Å). The two tyrosines are nearly perpendicular, a configuration often observed when two tyrosines each stack with two independent ssDNA bases (Burley and Petsko, 1985). Stacking of Y153 with base A15 of DNA flips out the terminal base of the duplex opposite the 3' base pair; the adjacent T14 forms a base pair with the 3' terminal nucleotide of the primer strand.

Although interaction of ssDNA with  $\beta$  is a crystal contact, superposition of the symmetry-related  $\beta$ -ssDNA protomer onto the structure shows very little gap between the two DNA molecules (Figure S3). Therefore, even though the  $\beta$ -ssDNA interaction in the crystal is intermolecular, the ssDNA would appear capable of binding intramolecularly to the protein-binding pocket in solution. If  $\beta$ -ssDNA interaction is functional, and not a crystal contact artifact, mutation of the surface tyrosines that stack with nucleotide bases should be defective in replication assays. Indeed, substitution of these tyrosines for serine significantly lowers the replication activity of  $\beta$ , and single substitutions result in intermediate effects (Figure 5A). Analysis of these mutants demonstrates that the defect lies in clamp loading, not polymerase speed (Figures 5B and 5C). The  $K_{ds}$  for interaction of these  $\beta$  tyrosine mutants to the clamp loader are minimal, 1.4- to 2.5-fold (Figure S2), and therefore interaction of  $\beta$  with ssDNA, as with dsDNA, likely plays a role in clamp loading at some point after initial substrate binding (see Discussion).

### DNA Competes with Pol III for the Protein-Binding Pocket of $\beta$

Next we developed an assay to test whether ssDNA uses the protein-binding pocket of  $\beta$  to interact with primed DNA. In this experimental design, we used a 9-mer peptide derived from the C terminus of the Pol III  $\alpha$  subunit, which is known to bind the hydrophobic pocket of the  $\beta$  clamp (Lopez de Saro et al., 2003). The cocrystal structure of  $\beta$  in complex with this Pol III 9-mer peptide shows that it localizes to the hydrophobic protein-binding pocket of  $\beta$  and does not interfere with DNA-binding residues R24, Q149, or those in the central cavity (R.E.G. and M.O. unpublished data). This is also the case in the cocrystal structure of *E. coli*  $\beta$  with a C-terminal peptide derived from Pol IV (Burnouf et al., 2004).

If  $\beta$  utilizes the protein-binding pocket to bind primed DNA, then the Pol III 9-mer peptide should compete with DNA binding to  $\beta$ . To examine this possibility,  $\beta$  was labeled with Alexa Fluor 555 ( $\beta^{AF555}$ ) and then was complexed with a primed DNA containing a 3' end-labeled quencher (see Figure 6). The AF555 emission spectrum overlaps the quencher absorption spectrum and is quenched by the labeled DNA. The concentrations of components were chosen to exploit the difference in affinity of  $\beta$  for primed DNA and dsDNA, such that  $\beta^{AF555}$ -DNA<sup>Quencher</sup> complex formation largely depends on the ssDNA interaction with  $\beta$ . If the ssDNA of the primed site binds to the protein-bind-

ing pocket of  $\beta$ , the Pol III 9-mer peptide should displace the ssDNA from the protein-binding pocket, causing the DNA<sup>Quencher</sup> to dissociate and restoring the fluorescence of  $\beta^{AF555}$ . The result, in Figure 6, shows an increase in  $\beta^{AF555}$  fluorescence as the Pol III 9-mer peptide is titrated into the assay, consistent with ssDNA binding to the protein-binding pocket of  $\beta$ .

## DISCUSSION

### $\beta$ Directly Interacts with DNA

The current study reveals that  $\beta$  binds DNA directly, independent of the ring shape of  $\beta$ . This is apparent from solution studies showing that  $\beta$  forms a saturable  $\beta$ -DNA complex with linear DNA at low concentration, but not with circular DNA (Figure 1). If  $\beta$  were to bind DNA only due to the ring shape of the clamp, it would slide off linear DNA rather than building up a substantial amount of  $\beta$ -DNA complex at equilibrium, especially at low concentrations. The conclusion that  $\beta$  binds DNA independent of its ring shape is supported by the fact that a  $\beta$  monomer mutant, which is no longer a ring, binds DNA (both linear and circular DNA) with the same affinity as WT  $\beta$ . This finding encouraged us to screen  $\beta$  and DNA for a  $\beta$ -DNA cocrystal.

### A Visual Screen for Cocrystals

We present here a simple method to screen oligonucleotide binding proteins for cocrystals containing the DNA (or RNA). The method employs a chromophoric tag on the DNA. Crystals containing bound DNA are deeply colored (e.g., Figure 2A and Figures S1B and S1C) and easily distinguished from crystals that lack DNA. In the present study, the DNA was 5' end labeled with either Cy5 or TAMN. This method is especially useful for proteins that bind weakly to an oligonucleotide substrate, as most conditions may not yield cocrystals, but would require time-consuming analysis to verify whether the ligand is present. This method also generalizes to other ligands besides DNA, as long as the ligands can be tagged without disrupting its ability to form a complex with the protein. For example, peptides tagged with a chromophore can be used to screen for conditions that yield protein-peptide cocrystals (e.g., Figure S1A).

### Arrangement of Primed DNA in $\beta$

The cocrystal structure reveals that  $\beta$  interacts with DNA such that the duplex is highly angled (22°) as it passes through the ring. Although the crystal contact made by the ssDNA could underlie or contribute to the angle of DNA, we note that recent molecular simulations predict that DNA can achieve a similar steep angle though the PCNA clamp (Ivanov et al., 2006). The  $\beta$  clamp also binds template ssDNA, which resides in a hydrophobic protein-binding pocket on the C-terminal face of the clamp. The ssDNA interaction is a crystal contact, which probably helps crystal growth, but it orients primed DNA through  $\beta$  in a direction that is the reverse of normal. We demonstrate here that ssDNA binds the hydrophobic pocket of  $\beta$  in solution and contributes

(C) Schematic of  $\beta$ -DNA interactions. Nucleotides are numbered in the standard way, starting with the 5' end of the primer strand and continuing with the 5' end of the template strand. The residues of  $\beta$  that interact with DNA (cutoff, 4.5 Å) are marked in red (protomer A) or blue (protomer B); residues in gray belong to the symmetry-related  $\beta$  molecule. Color assignment of nucleotide bases are as follows: dT, blue; dA, red; dC, green; and dG, yellow. The gray icon surrounding residue 11 represents the binding pocket of the symmetry-related  $\beta$  molecule. The underlined residues represent polypeptide backbone interactions with the DNA.

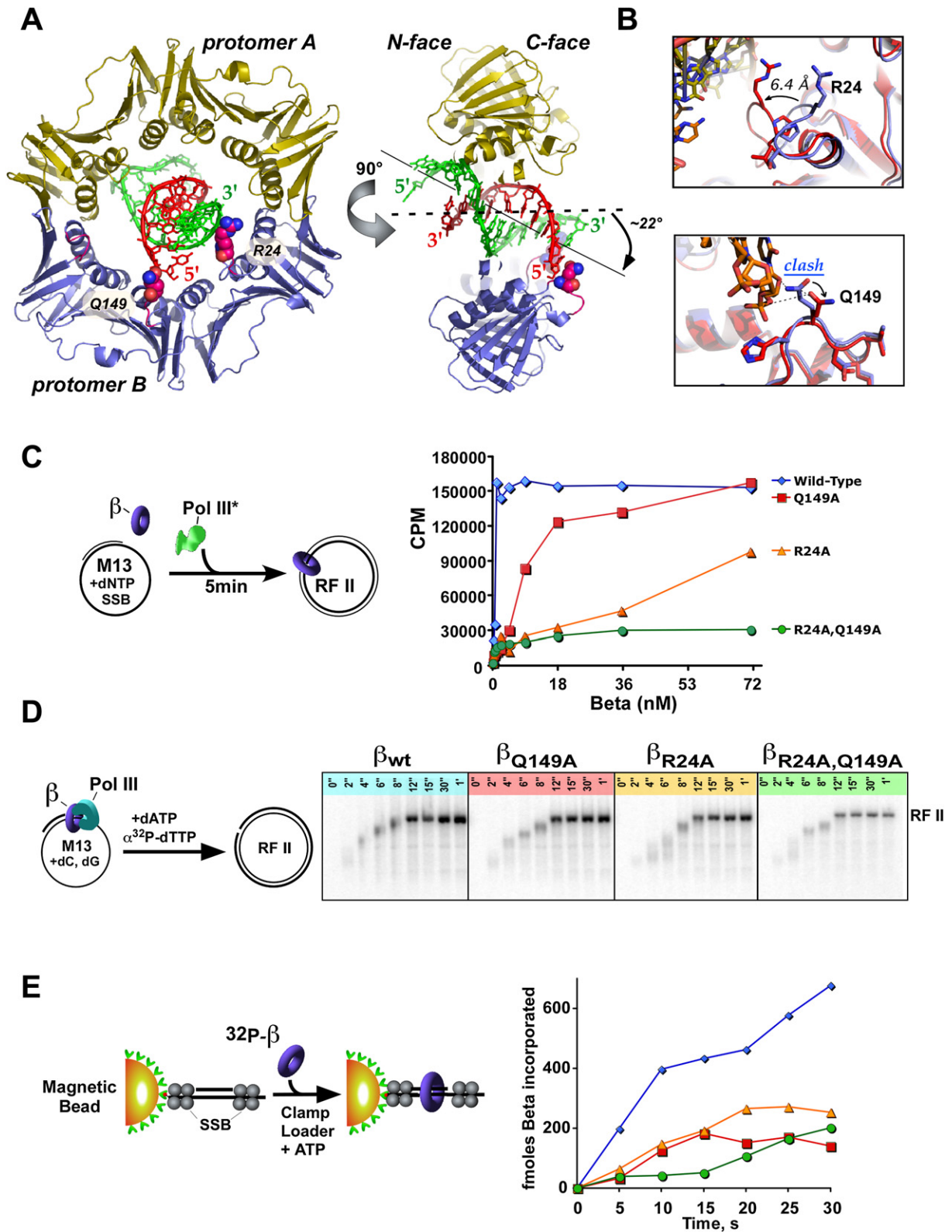


**Figure 3. Structure of the  $\beta$ -DNA Complex**

(A) Ribbon representation of the  $\beta$ -DNA complex: front and side views. DNA is tilted  $\sim 22^\circ$  from the C2 rotation axis of  $\beta$ . The Cy5 moiety is not shown for clarity but is shown in Figure S4.



to clamp loading activity, indicating that this contact is intramolecular and the primed DNA is correctly oriented through  $\beta$  in solution. The evidence that the  $\beta$ -ssDNA contact is physiologically relevant is as follows. First, primed DNA binds to  $\beta$  about 4-fold tighter than dsDNA, implying that ssDNA unique to the primed site interacts with  $\beta$ . Second, mutation of the tyrosines that bind ssDNA significantly reduce replication activity and clamp loading rate, indicating that  $\beta$ -ssDNA interaction is functional. And third, a Pol III peptide that binds the hydrophobic pocket of  $\beta$  competes with primed DNA for  $\beta$ , indicating that DNA binds the hydrophobic protein-binding site of  $\beta$ . Because the biochemical studies are performed in dilute solution, we presume primed DNA transits through the  $\beta$  clamp in the physiologically relevant orientation, enabling ssDNA to bind the protein-binding pocket (see illustrations in Figures 6 and 7).

One may presume that, during function with DNA polymerase, the polymerase will bind the protein-binding site of  $\beta$  and displace ssDNA from  $\beta$  (see Figure 7B). Because the polymerase- $\beta$  clamp complex must move on DNA, we expect that the several direct connections of  $\beta$  to DNA we observe here (Figure 2C) are transient and easily broken, enabling the clamp to slide on DNA during function with polymerase. In the dynamic situation of  $\beta$ -polymerase function, DNA likely adopts many different conformations as it passes through  $\beta$ , besides the view shown in the cocrystal structure.

### $\beta$ -DNA Interaction Plays a Role in Clamp Loading

Mutation of residues in  $\beta$  that bind ssDNA and/or dsDNA show defects in the clamp loading step; polymerase elongation speed is not affected. These  $\beta$  mutants bind the clamp loader with nearly the same affinity of WT  $\beta$  (Figure S2), and therefore the role of  $\beta$ -DNA binding appears to lie in the clamp loading mechanism at a step downstream of initial clamp-clamp loader complex formation.

Where in the clamp loading mechanism may clamp residues that bind DNA be important to function? One possibility is illustrated in Figure 7A. The initial clamp loading intermediate that builds up prior to ATP hydrolysis consists of an open clamp in the form of a spiral that matches the spiral clamp loading AAA+ domains of the five clamp loader subunits (Figure 7A, first diagram) (reviewed in Bloom, 2006). This open clamp-clamp loader-ATP complex binds primed DNA and positions it through the open clamp. We propose that, once DNA is positioned inside the clamp, the DNA interactive residues of the clamp are attracted to DNA and induce the clamp to close around DNA (Figure 7A, middle diagram). The clamp, in transiting from an open spiral to a closed planar structure (and tilted), no longer matches the spiral surface of the clamp loader, thereby breaking its connection to some of the clamp loading subunits. The strongest  $\beta$  clamp loading subunit interaction is mediated by the  $\delta$  subunit of the clamp

loader, which binds the protein-binding pocket of  $\beta$  (Jeruzalmi et al., 2001). Hence, template ssDNA binding to the protein-binding pocket of  $\beta$  may help release  $\delta$  from  $\beta$  and thereby complete clamp loader ejection, a necessary prerequisite for polymerase to bind  $\beta$  (Figure 7A, right diagram) (Naktinis et al., 1996).

### The $\beta$ -ssDNA Contact May Act as a “Placeholder”

After the clamp loader dissociates from  $\beta$ , the clamp may remain at the primed site through its connection to template ssDNA (Figure 7B). In the absence of this connection,  $\beta$  could slide away from the 3' terminus. Thus the  $\beta$ -ssDNA connection may serve a “placeholder” role, keeping  $\beta$  at the primed site where it is needed for function with DNA polymerase. Pol III contains two regions that bind to  $\beta$  (Dohrmann and McHenry, 2005; Lopez de Saro et al., 2003). Because polymerase competes with ssDNA for the protein-binding pocket of  $\beta$  (i.e., Figure 6), the  $\beta$ -ssDNA interaction will be broken upon association of polymerase with  $\beta$ , and this may facilitate  $\beta$  diffusion along DNA. A placeholder function also has implications for how multiple factors may switch on the clamp, as described below.

### The Angle of DNA through $\beta$ Has Implications for DNA Switching

Another possible role of  $\beta$ -DNA interaction observed here is implied by the highly tilted orientation of DNA as it passes through the ring.  $\beta$  is a homodimer and thus has two identical protein-binding sites, enabling it to bind two different proteins at once. This has been demonstrated directly for Pol III and Pol IV binding to  $\beta$  and may generalize to other  $\beta$  interactive factors (Indiani et al., 2005; Sutton, 2004). Two DNA polymerases that bind one  $\beta$  clamp must vie for the single primed terminus.

The structure of the  $\beta$ -DNA complex shows that DNA is steeply angled through the ring, and this presents a possible route by which DNA may switch among two different proteins bound to the same clamp. The reasoning is as follows. DNA interactive residues R24 and Q149 are “off center” relative to the circular clamp and are located on loops of the face of the clamp to which proteins bind. Thus these residues likely contribute to the tilted orientation of DNA through the center of the ring. Because  $\beta$  is a homodimer, the DNA should partition equally among two orientations in which it contacts R24/Q149 of one protomer or the other (e.g., see Figure 7C). Tilted DNA that switches between two protomers within one clamp may facilitate switching of the DNA between two different DNA polymerases bound to the same  $\beta$  clamp, thus relocating from the active site of one DNA polymerase to the active site of the other. Interestingly, PCNA from the archaeon *Sulfolobus solfataricus* is a heterotrimer and each protomer binds a different protein (DNA polymerase, flap endonuclease, and DNA ligase) (Dionne et al., 2003), and switching among the different factors may be facilitated by DNA movements inside the ring,

(B) Detailed view of R24 (top) and Q149 (bottom) in the  $\beta$ -DNA complex compared to the apo  $\beta$  structure (blue).

(C) Replication assays using primed M13 ssDNA coated with SSB contain Pol III\* and the indicated amount of either WT  $\beta$  (blue diamonds),  $\beta_{Q149A}$  (red squares),  $\beta_{R24A}$  (orange triangles), or  $\beta_{R24A/Q149A}$  (green circles).

(D) Polymerase extension rate was determined with primed M13 ssDNA to which  $\beta$ , or mutant  $\beta$ , is first assembled on the DNA, followed by initiating synchronous chain extension. Reactions were quenched at the indicated times, and products were analyzed in a native agarose gel.

(E) The scheme illustrates the bead conjugated primed DNA in which SSB blocks  $^{32}P$ - $\beta$  from sliding off the end of the DNA. Clamp loading rate was assessed in assays with either  $\beta_{WT}$  (blue),  $\beta_{Q149A}$  (red),  $\beta_{R24A}$  (orange), or  $\beta_{R24A,Q149A}$  (green).

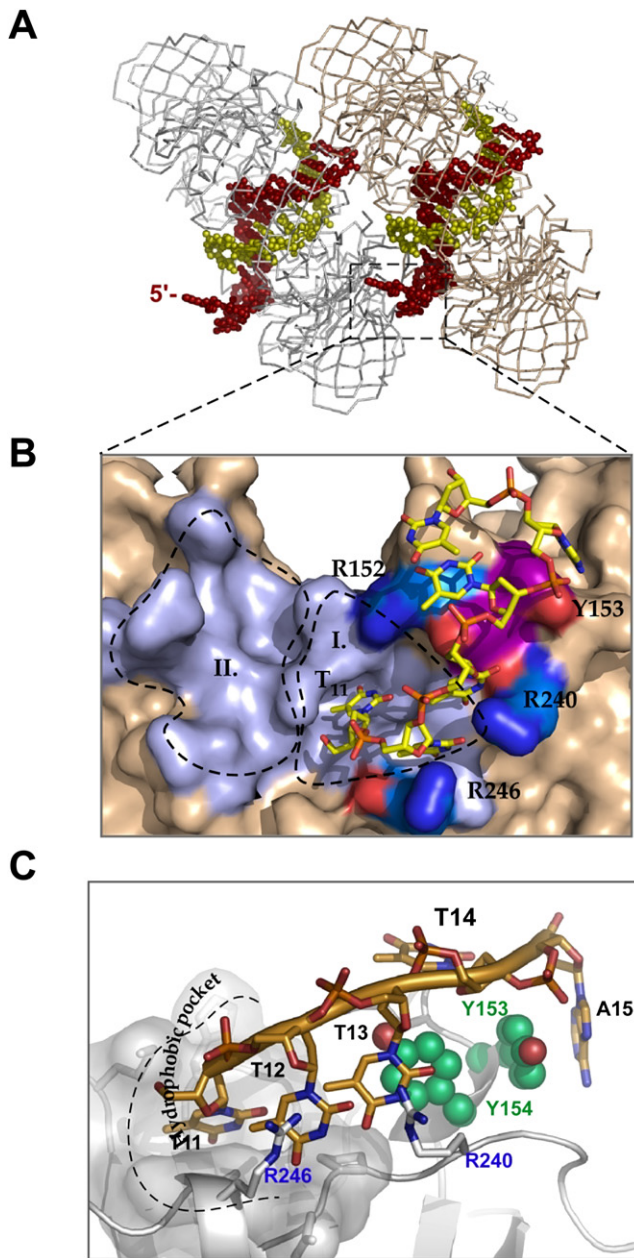


**Figure 4. Interaction of  $\beta$  with the ssDNA Region of the Primed Site**

(A) Crystal lattice showing two molecules of the  $\beta$ -DNA complex. The ssDNA makes a crystal contact between two molecules of  $\beta$ .

(B) Surface representation of the charged residues that line the channel directing ssDNA to the hydrophobic protein-binding site of  $\beta$ . Basic residues are colored blue. The protein-binding site is shaded purple and subsites I and II (defined in Burnouf et al., 2004) are indicated.

(C) View of ssDNA (orange) positioned inside the hydrophobic protein-binding pocket of  $\beta$ . Thy<sub>11</sub> and Thy<sub>12</sub> occupy subsite I of the  $\beta$  hydrophobic pocket; the exposed R246, R240 side chains interact with the DNA phosphate backbone. Y153 and Y154 (green) stack with Ade<sub>15</sub> and Thy<sub>13</sub>, respectively.

as proposed above for *E. coli*  $\beta$ . DNA switching among different proteins attached to the same ring has also been proposed in molecular simulation studies of PCNA (Ivanov et al., 2006).

Many proteins bind to the  $\beta$  clamp. For example,  $\beta$  binds all five *E. coli* DNA polymerases and also MutS, MutL, Had, and ligase. The damage-inducible polymerases, Pols II, IV, and V, are less accurate than Pol III and are thought to traverse certain lesions that would otherwise block replication fork progression (Goodman, 2002; Fujii and Fuchs, 2004). These polymerases are thought to utilize overlapping sites on  $\beta$  and switch among themselves when Pol III stalls, thereby allowing different polymerases to “sample”  $\beta$  in a process called “replication fork management” (Sutton et al., 2000; Sutton and Walker, 2001; Maul et al., 2007; Sutton and Duzen, 2006). The ability of  $\beta$  to bind template ssDNA may also facilitate switching of different proteins on  $\beta$ . For example, when the stalled Pol III dissociates from the primed site,  $\beta$  may bind ssDNA to remain at the ss/ds junction, and this may increase the association of an error-prone polymerase with  $\beta$  for advancing the fork past a template block.

Intracellular importance of DNA binding to  $\beta$  is provided by the *dnaN159* mutant of  $\beta$ , which shows pleiotropic defects in DNA replication and repair (Sutton, 2004; Sutton and Duzen, 2006). The *dnaN159* mutant of  $\beta$  carries two amino acid changes, G66E and G174A, and the crystal structure shows one of these residues, G174, binds DNA. Study of a G174A  $\beta$  mutant reveals altered relative affinity of Pol II, Pol IV, and Pol V for  $\beta$  compared to Pol III (Maul et al., 2007; Sutton and Duzen, 2006). These studies are consistent with the view that different polymerases have only partly overlapping binding sites on the  $\beta$  clamp and suggest that DNA interaction near the polymerase-binding site(s) on  $\beta$  facilitates exchange of different polymerases on  $\beta$ .

#### Implications for Eukaryotic PCNA

Does eukaryotic PCNA form contacts to DNA, like *E. coli*  $\beta$ ? We have used chromophoric-tagged DNA structures in cocrystal trials with yeast PCNA and observe deeply colored crystals (Figure S1B). The fact that PCNA-DNA cocrystals can be formed indicates that PCNA may bind DNA in a specific fashion, as observed here for the *E. coli*  $\beta$ -DNA complex. In support of this proposal are recent molecular simulations of PCNA that indicate DNA can achieve an angle as steep as 20° through PCNA (Ivanov et al., 2006). Furthermore, like  $\beta$ , PCNA contains hydrophobic protein-binding pockets on the C-terminal face of the clamp. Perhaps PCNA binds ssDNA in these protein-binding sites, as demonstrated here for *E. coli*  $\beta$ . Whether DNA forms direct contacts to PCNA and, if so, whether they are involved in clamp loading, must await future studies.

The fact that  $\beta$  binds both the dsDNA and ssDNA of a 3' primed site junction suggests that  $\beta$  may help determine specificity of clamp loading at a 3' ss/ds junction relative to loading at a 5' ss/ds junction. In this regard, it is interesting to note that the eukaryotic RFC clamp loader has alternative forms, one of which loads a different clamp. The different clamps, PCNA and 9-1-1, are loaded onto either the 3' or 5' terminus of a ss/ds junction, respectively (Ellison and Stillman, 2003; Yao et al., 2000). Considering that  $\beta$  binds both dsDNA and ssDNA of a primed site, it is tempting to speculate that some of the directionality in clamp loading may be inherent in the clamp. Future studies of these issues are sure to yield exciting insights into these important cellular processes.



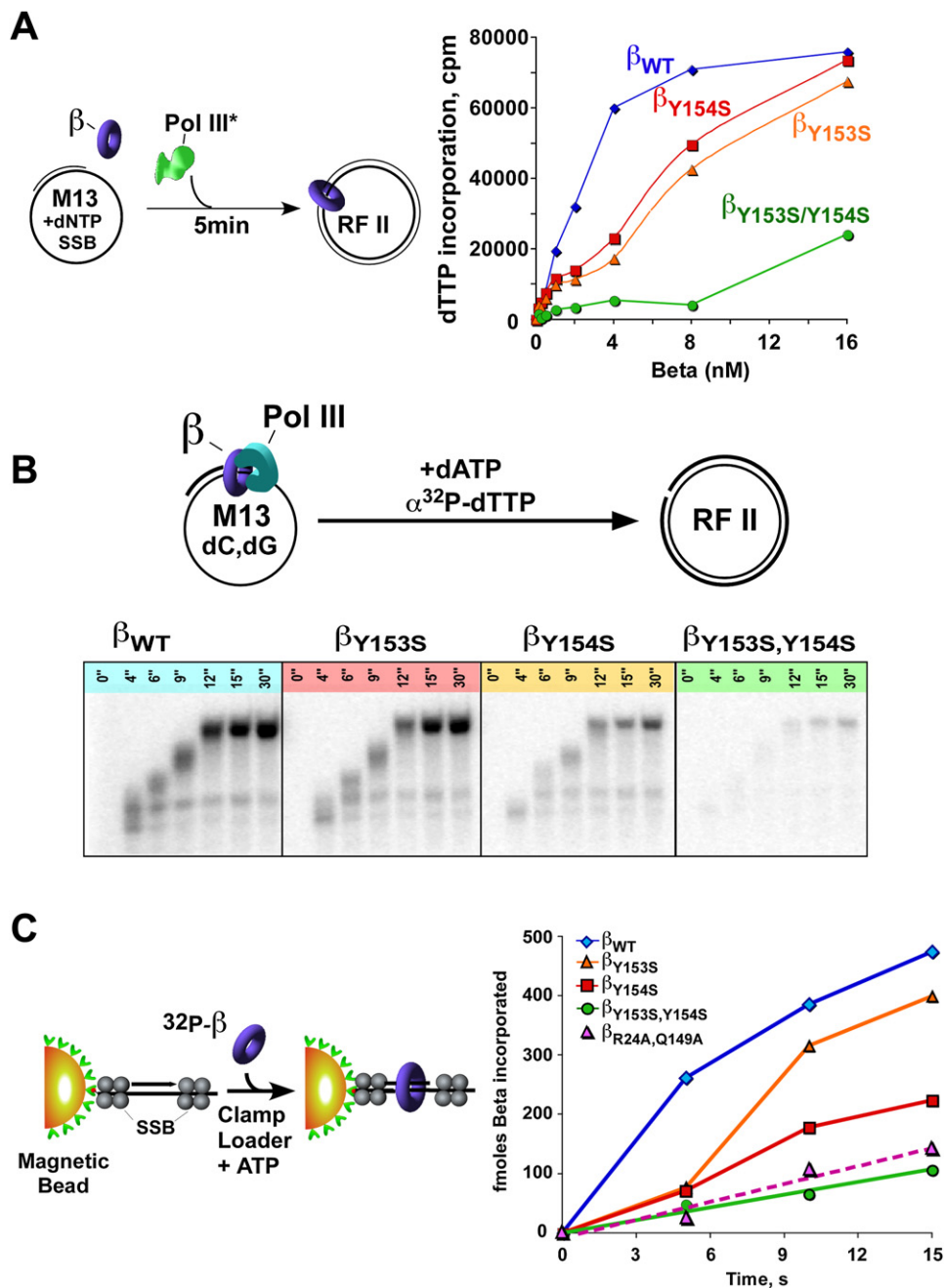


### Figure 5. The ssDNA Binding Tyrosines of $\beta$ Are Important to Function

(A) Replication assays contain the indicated amount of Pol III\* and  $\beta$  (or mutant  $\beta$ ). The plot shows the quantitation of DNA synthesis with either  $\beta_{WT}$  (blue diamonds),  $\beta_{Y154A}$  (red squares),  $\beta_{Y153A}$  (orange triangles), or  $\beta_{Y154A/Y153A}$  (green circles).

(B) Polymerase extension rate was determined with primed M13 ssDNA to which  $\beta$ , or mutant  $\beta$ , is assembled on the DNA followed by initiating synchronous chain extension and native agarose gel analysis of products after quenching at the indicated times.

(C) Bead-based clamp loading rate assays were performed with either  $\beta_{WT}$  (blue),  $\beta_{Y154A}$  (red),  $\beta_{Y153A}$  (orange), or  $\beta_{Y154A/Y153A}$  (green). For the purpose of comparison, the purple squares are the result with  $\beta_{R24A,Q149A}$ .

Despite the many proposals of clamp-DNA interactions discussed here, further studies are needed to document the roles of the various  $\beta$ -DNA contacts that occur during its dynamic function. The current study demonstrates that direct clamp-

DNA contacts are involved in the clamp loading step, possibly in helping the clamp to close around DNA. Whether direct clamp-to-DNA contacts also serve as a placeholder to keep the clamp the primed site to help mediate polymerase switching

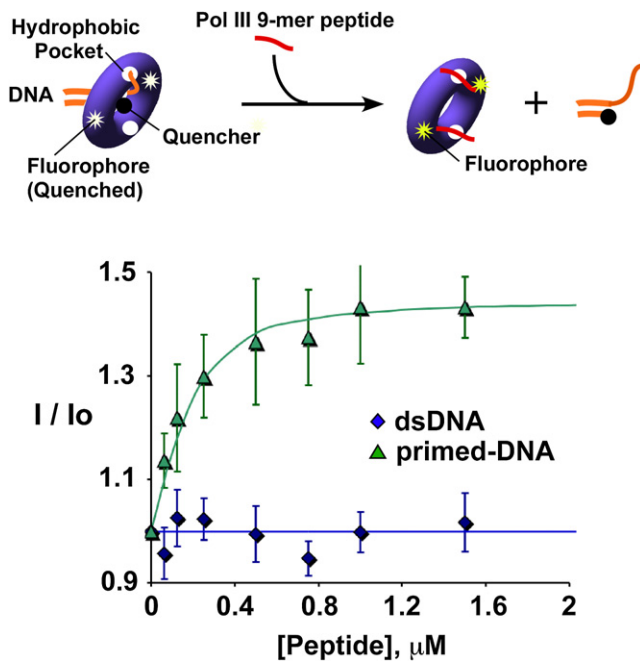


**Figure 6. Pol III C-Terminal 9-mer Peptide Competes with Primed Template ssDNA**

The scheme illustrates the experimental design. Fluorescent  $\beta^{\text{AF555}}$  is bound to primed DNA containing a quencher. A 9-mer Pol III  $\alpha$ -C-terminal peptide binds to the hydrophobic pocket of  $\beta$ . Therefore, if ssDNA occupies the same site, addition of the Pol III 9-mer peptide should displace the quencher-DNA and result in recovery of  $\beta^{\text{AF555}}$  fluorescence. The result indicates that the 9-mer Pol III peptide results in recovery of  $\beta^{\text{AF555}}$  fluorescence (green triangles) and thus competes with primed DNA for the hydrophobic pocket. Use of a blunt duplex with a quencher forms a small amount of  $\beta$ -DNA complex under these conditions but is not affected by addition of 9-mer peptide (blue diamonds). This indicates that peptide competes with ssDNA, which is only present on the primed site. The error bars are the standard deviation of five experiments, and the symbol is placed at the average.

or whether the tilt of DNA through  $\beta$  is maintained and used to aid switching among multiple clamp factors bound simultaneously to the same clamp are important topics for future studies.

## EXPERIMENTAL PROCEDURES

### Materials

Labeled nucleotides are from Dupont-NEN, and unlabeled nucleotides are from Pharmacia-LKB. Streptavidin-coated Dynabead M-280 magnetic beads are from Dynal Biotech. Primed templates labeled with Cy-5 or TAMN were from Integrated DNA Technologies (Coralville, IA): Primers, 5'-Cy5/CCCATCGTAT-3', 5'-TAMN56/CCCATCGTAT-3'; templates, 5'-[T<sub>n</sub>]ATACgATggg-3'. To yield 10/10-, 10/12-, 10/14-, 10/16-, 10/18-, and 10/20-mer primed templates, oligonucleotides were annealed by using equimolar ratios with 10 mM Tris-HCl, 1 mM EDTA (pH 7.8). Magnetic bead clamp loading assays used a 30-mer (5'-gCAATAACTggCCgTTTgAAgATTTcG-3'), and 3' biotinylated 102-mer (5'-CCA TTCTgTAACgCCAgggTTTTTcGcAgTCAACATTCgAAATCTTCAAACgACggCC AgTTATTgCTCTTCTTgAgTTTgATAgCCAAAACgACCATTATAg/TEGBiotin/-3') annealed 2:1. M13mp18 ssDNA was primed with a DNA 60-mer.  $\beta$  and SSB were purified as described (Kong et al., 1992). Pol III\*, Pol III core, and  $\gamma$  complex were reconstituted as described (McInerney and O'Donnell, 2004).

### $\beta$ Mutants

The *dnaN* gene encoding  $\beta$  was cloned into a modified pET16c vector, which incorporates a short N-terminal hexahistidine and protein kinase tag (Stukenberg et al., 1994). Single and double  $\beta$  mutants ( $\beta_{\text{Q149A}}$ ,  $\beta_{\text{R24A}}$ ,  $\beta_{\text{R24A/Q149A}}$ ,  $\beta_{\text{Y153A}}$ ,  $\beta_{\text{Y154A}}$ , and  $\beta_{\text{Y153A/Y154A}}$ ) were constructed by the QuikChange XL protocol (Stratagene Inc.). Plasmids were introduced into *E. coli* BL21[DE3] and grown in LB to OD 0.6 at 37°C, then lowered to 20°C and induced upon adding 0.1 mM IPTG followed by incubation at 20°C for 10 hr. The  $\beta$  monomer mutant ( $\beta_{\text{I272A/L273A}}$ ) was as described (Jeruzalmi et al., 2001).

### Data Acquisition and Structure Refinement

Conditions for cocystal formation were 0.2 mM  $\beta$  dimer and 0.22 mM DNA in 10 mM Tris-Cl (pH 7.4), 50 mM NaCl, 0.5 mM EDTA, and 10% glycerol. Protein-DNA solutions were mixed with an equal volume of 22%–26% PEG 400, 75 mM MES (pH 5.9), 75 mM CaCl<sub>2</sub>, 5% glycerol, and 0.5% DMSO and allowed to equilibrate by vapor diffusion. Crystals grew to approximate dimensions (0.2 × 0.3 × 0.3 mm<sup>3</sup>) in 2 weeks at room temperature.

Diffraction data were collected at 100K at the X4a beamline at the National Synchrotron Light Source, Brookhaven National Laboratory. Data were indexed and scaled with the HKL2000 program suite (Otwinowski and Minor, 1997). A data set of 1.61 Å resolution was collected for the uncomplexed  $\beta$ , and the structure was solved by molecular replacement using the known  $\beta$  structure (Kong et al., 1992) and refined to 1.7 Å with CNS (Brunger et al., 1998) (see Table S1).

Crystals of  $\beta$ -DNA complex diffracted to 1.92 Å resolution, and the structure was solved by molecular replacement using the newly refined native structure as the search model. Refinement was initiated by placing a 10 bp duplex DNA with ideal B type geometry built with ICM-Pro (Molsoft L.L.C.). The  $\beta$ -DNA structure was refined without placing any restraints on the DNA duplex. Changes in the  $\beta$ -DNA complex structure were made by using the program O (Jones et al., 1991). All refinements were carried out against  $|F_0| > 0\sigma$  data, using the CNS program suite (Brunger et al., 1998). The final model spans all protein residues (2 × 366 residues) and the entire primed-DNA template.

### M13mp18 ssDNA Extension Assays

#### $\beta$ Clamp Dependence

$\beta$  (0, 15, 31, 62, 124, 248, 494, 988, and 1975 fmol) was incubated with SSB (425 pmol) and primed M13mp18 ssDNA (30 fmol) for 5 min at 37°C in 25  $\mu\text{l}$  of replication buffer (25 mM TrisCl [pH 7.5], 5 mM DTT, 40  $\mu\text{g/ml}$  BSA, 4% glycerol, 8 mM MgCl<sub>2</sub>, and 0.5 mM ATP) containing 60  $\mu\text{M}$  each dGTP, dCTP, dATP, and 20  $\mu\text{M}$  [ $\alpha$ -<sup>32</sup>P]dTTP. DNA synthesis was initiated upon adding Pol III\* (100 fmol). After 2 min, reactions were quenched with 25  $\mu\text{l}$  of 1% SDS/40 mM EDTA. One-half of the reaction was spotted on DE81 filters to quantitate DNA synthesis, while the other half was analyzed in a 0.8% neutral agarose gel.

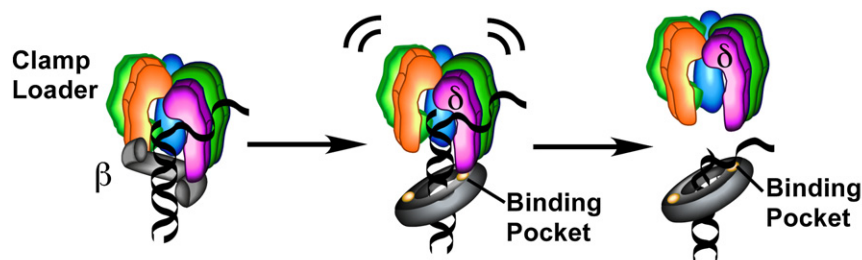
#### Pol III- $\beta$ Rate of Synthesis Measurements

$\beta$  was assembled onto primed M13mp18 ssDNA coated with SSB in 25  $\mu\text{l}$  of replication buffer containing  $\beta$  (450 fmol), SSB (425 pmol),  $\gamma$  complex (20 fmol), primed M13mp18 ssDNA (30 fmol), 0.5 mM ATP, and 8 mM MgCl<sub>2</sub>. Pol III core (850 fmol) and 60  $\mu\text{M}$  each dGTP and dCTP were added, followed by incubation for 10 min at 37°C. DNA synthesis was initiated upon adding 60  $\mu\text{M}$  dATP and 20  $\mu\text{M}$  [ $\alpha$ -<sup>32</sup>P] dTTP. After 2, 4, 6, 8, 15, 30, or 60 s, reactions were quenched and analyzed as above.

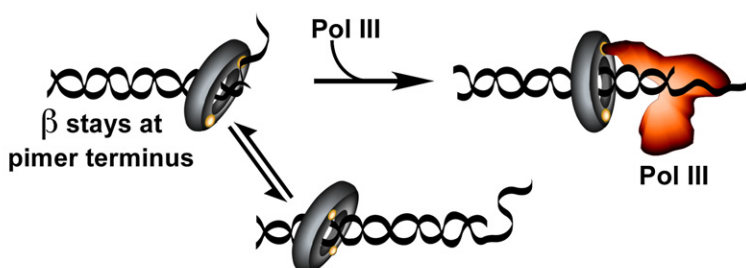
#### Clamp Loading Assay

The 30/102-mer biotinylated DNA was conjugated to M-280 Streptavidin Dynabeads in 10 mM Tris-HCl (pH 7.5), 1 mM EDTA, 150 mM NaCl, and 5 mg/ml BSA at 22°C for 30 min and washed three times with the same buffer. The yield was 185 ± 35 pmol of DNA/mg of Dynabeads. Clamp loading was performed at 20°C in clamp loading buffer (30 mM Tris-HCl [pH 7.5], 7 mM Mg[OAc]<sub>2</sub>, 100 mM NaCl, 1 mM DTT, and 1 mM CHAPS) containing 1 mM ATP, 280 nM DNA, 600 nM *E. coli* SSB (tetramer), and 140 nM (dimer) <sup>32</sup>P- $\beta^{\text{HK}}$  (or <sup>32</sup>P- $\beta^{\text{HK}}$  mutants). Reactions were incubated 1 min, then initiated by adding 70 nM  $\gamma$  complex and quenched with 21 mM EDTA (pH 7.5) at the indicated times. Beads were harvested in a magnetic concentrator and washed twice in clamp loading buffer containing 200 mM NaCl. Protein was stripped from beads by using 1% SDS at 95°C for 5 min. <sup>32</sup>P- $\beta^{\text{HK}}$  was quantified by liquid scintillation and visually verified in a 12% SDS-PAGE.

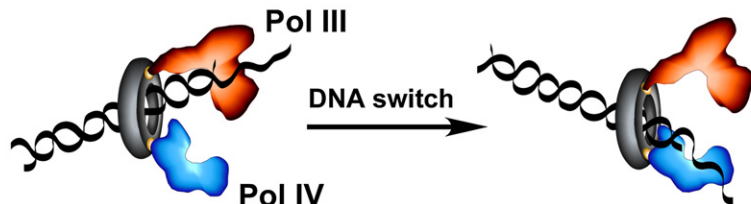
## A DNA helps $\beta$ close during clamp loading



## B Placeholder for Pol III



## C DNA tilt helps switching among polymerases



### $K_d$ Measurements of $\beta$ - $\gamma$ Complex Interaction

WT  $\beta$  and  $\beta$  mutants were labeled with pyrene maleimide (Molecular Probes, Inc., Eugene, OR) to form  $\beta^{Py}$  as described (Snyder et al., 2004). Reactions contained  $\beta^{Py}$  (50 or 100 nM) in 60  $\mu$ l 20 mM Tris-Cl (pH 7.5), 8 mM  $MgCl_2$ , 1 mM DTT, 0.2 mM EDTA, 50 mM NaCl, and 0.5 mM ATP or ATP- $\gamma$ S.  $\beta^{Py}$  anisotropy is enhanced upon  $\gamma$  complex binding. Titrations and  $K_d$  measurements were performed as described (Anderson et al., 2007).

### $K_d$ Measurements of $\beta$ -DNA Binding

WT  $\beta$  and  $\beta$  mutants were labeled with OregonGreen488 maleimide (Molecular Probes, Inc., Eugene, OR) to form  $\beta^{OG}$  as described (Lopez de Saro et al., 2003). The following oligonucleotides were used to construct 18/18-mer blunt duplex and 18/28-mer 3' primed template: 5'-CCCATCgTATAGCAAggg-3' (18-mer primer), 5'-CCCTTgCTATACgATggg-3' (18-mer template), and 5'-TTTTTTTTCCCTTgCTATACgATggg-3' (28-mer template). DNA titrations contained  $\beta^{OG}$  (200 or 500 nM) in 60  $\mu$ l of 20 mM Tris-Cl (pH 7.5), 1 mM DTT, 0.2 mM EDTA, and 40 mM NaCl. Reactions were equilibrated at 22°C for 10 min and then transferred into a 3  $\times$  3 mm cuvette. Fluorescence emission spectra were recorded from 500 to 630 nm (excitation at 490 nm); emission at 517 nm was used for analysis.

### Peptide Competition Experiments

$\beta$  was modified with an AF555 fluorophore (Molecular Probes) to yield  $\beta^{AF555}$  as described above for  $\beta^{OG}$ .  $\beta^{AF555}$  (150 nM) was mixed with an 18/34-mer primed DNA labeled at the 3' terminus of the 18-mer with a Black Hole quencher (IDT)

### Figure 7. Possible Functions of $\beta$ -DNA Contacts

(A) Proposed role of DNA binding during the clamp loading reaction. Left diagram, the clamp loader subunits form a spiral surface that binds an open clamp, twisting it into a lockwasher configuration. Primed DNA is attracted inside the circular clamp loader, thereby positioning DNA through the ring. Middle diagram, attractive contacts between  $\beta$  and DNA induces the clamp to close around DNA. The planar closed ring no longer matches the spiral shape of the clamp loader, thereby disconnecting  $\beta$  from clamp loader subunits. Right diagram, template ssDNA binds the hydrophobic pocket of  $\beta$ , displacing  $\delta$  subunit and completing the clamp loading reaction.

(B) Proposed "placeholder" role for  $\beta$ -ssDNA contact. The contact between the template ssDNA and protein-binding pocket of  $\beta$  may hold it near the 3' terminus of DNA. Pol III connects to both protein-binding sites on  $\beta$ . Thus, Pol III binding likely displaces ssDNA from the protein-binding pocket of  $\beta$ , and this may release  $\beta$  from the ssDNA template for sliding on dsDNA.

(C) Proposed role of DNA tilt in polymerase switching on  $\beta$ . Because  $\beta$  consists of two identical protomers, the DNA may alternate from one to the other, facilitating interaction with different DNA polymerases bound to the same clamp.

in 60  $\mu$ l of 20 mM Tris-HCl (pH 7.5), 1 mM DTT, 0.2 mM EDTA, and 40 mM NaCl. A 9-mer peptide corresponding to the C terminus of Pol III  $\alpha$  subunit was titrated into the reaction. A control experiment between the free AF555 fluorophore and the Black Hole-labeled primed template showed no quenching.

### Supplemental Data

Supplemental Data include four figures and one table and can be found with this article online at <http://www.cell.com/cgi/content/full/132/1/43/DC1/>.

### ACKNOWLEDGMENTS

We are grateful to the staff at Brookhaven National Laboratory for their help, Jeff Finkelstein (Rockefeller U., NY) for technical assistance, and Daniel Barsky (LLNL, Lawrence, CA) and Lance Langston (Rockefeller U., NYC) for critically reading the manuscript. This work was supported by grants from the NIH, GM38839 (M.O.), GM70841 (X-P.K.), and GM45547 (J.K.).

Received: May 11, 2007

Revised: October 3, 2007

Accepted: November 30, 2007

Published: January 10, 2008

### REFERENCES

- Anderson, S.G., Williams, C.R., O'Donnell, M., and Bloom, L.B. (2007). A function for the chi subunit in loading the Escherichia coli DNA polymerase sliding clamp. *J. Biol. Chem.* 282, 7035–7045.
- Argiriadi, M.A., Goedken, E.R., Bruck, I., O'Donnell, M., and Kuriyan, J. (2006). Crystal structure of a DNA polymerase sliding clamp from a Gram-positive bacterium. *BMC Struct. Biol.* 6, 2.



- Bloom, L.B. (2006). Dynamics of loading the *Escherichia coli* DNA polymerase processivity clamp. *Crit. Rev. Biochem. Mol. Biol.* *41*, 179–208.
- Brunger, A.T., Adams, P.D., Clore, G.M., DeLano, W.L., Gros, P., Grosse-Kunstleve, R.W., Jiang, J.S., Kuszewski, J., Nilges, M., Pannu, N.S., et al. (1998). Crystallography & NMR system: a new software suite for macromolecular structure determination. *Acta Crystallogr. D Biol. Crystallogr.* *54*, 905–921.
- Bunting, K.A., Roe, S.M., and Pearl, L.H. (2003). Structural basis for recruitment of translesion DNA polymerase Pol IV/DinB to the beta-clamp. *EMBO J.* *22*, 5883–5892.
- Burley, S.K., and Petsko, G.A. (1985). Aromatic-aromatic interaction: a mechanism of protein structure stabilization. *Science* *229*, 23–28.
- Burnouf, D.Y., Olieric, V., Wagner, J., Fujii, S., Reinbolt, J., Fuchs, R.P., and Dumas, P. (2004). Structural and biochemical analysis of sliding clamp/ligand interactions suggest a competition between replicative and translesion DNA polymerases. *J. Mol. Biol.* *335*, 1187–1197.
- Chapados, B.R., Hosfield, D.J., Han, S., Qiu, J., Yelent, B., Shen, B., and Tainer, J.A. (2004). Structural basis for FEN-1 substrate specificity and PCNA-mediated activation in DNA replication and repair. *Cell* *116*, 39–50.
- Dalrymple, B.P., Kongsuwan, K., Wijffels, G., Dixon, N.E., and Jennings, P.A. (2001). A universal protein-protein interaction motif in the eubacterial DNA replication and repair systems. *Proc. Natl. Acad. Sci. USA* *98*, 11627–11632.
- Dionne, I., Nookala, R.K., Jackson, S.P., Doherty, A.J., and Bell, S.D. (2003). A heterotrimeric PCNA in the hyperthermophilic archaeon *Sulfolobus solfataricus*. *Mol. Cell* *11*, 275–282.
- Dohrmann, P.R., and McHenry, C.S. (2005). A bipartite polymerase-processivity factor interaction: only the internal beta binding site of the alpha subunit is required for processive replication by the DNA polymerase III holoenzyme. *J. Mol. Biol.* *350*, 228–239.
- Ellison, V., and Stillman, B. (2003). Biochemical characterization of DNA damage checkpoint complexes: clamp loader and clamp complexes with specificity for 5' recessed DNA. *PLoS Biol.* *1*, E33. 10.1371/journal.pbio.0000033.
- Fujii, S., and Fuchs, R.P. (2004). Defining the position of the switches between replicative and bypass DNA polymerases. *EMBO J.* *23*, 4342–4352.
- Goodman, M.F. (2002). Error-prone repair DNA polymerases in prokaryotes and eukaryotes. *Annu. Rev. Biochem.* *71*, 17–50.
- Gulbis, J.M., Kelman, Z., Hurwitz, J., O'Donnell, M., and Kuriyan, J. (1996). Structure of the C-terminal region of p21(WAF1/CIP1) complexed with human PCNA. *Cell* *87*, 297–306.
- Indiani, C., McInerney, P., Georgescu, R., Goodman, M.F., and O'Donnell, M. (2005). A sliding-clamp toolbelt binds high- and low-fidelity DNA polymerases simultaneously. *Mol. Cell* *19*, 805–815.
- Ivanov, I., Chapados, B.R., McCammon, J.A., and Tainer, J.A. (2006). Proliferating cell nuclear antigen loaded onto double-stranded DNA: dynamics, minor groove interactions and functional implications. *Nucleic Acids Res.* *34*, 6023–6033.
- Jeruzalmi, D., Yurieva, O., Zhao, Y., Young, M., Stewart, J., Hingorani, M., O'Donnell, M., and Kuriyan, J. (2001). Mechanism of processivity clamp opening by the delta subunit wrench of the clamp loader complex of *E. coli* DNA polymerase III. *Cell* *106*, 417–428.
- Johnson, A., and O'Donnell, M. (2005). Cellular DNA replicases: components and dynamics at the replication fork. *Annu. Rev. Biochem.* *74*, 283–315.
- Jones, T.A., Zou, J.Y., Cowan, S.W., and Kjeldgaard, M. (1991). Improved methods for building protein models in electron density maps and the location of errors in these models. *Acta Crystallogr. A* *47*, 110–119.
- Kong, X.P., Onrust, R., O'Donnell, M., and Kuriyan, J. (1992). Three-dimensional structure of the beta subunit of *E. coli* DNA polymerase III holoenzyme: a sliding DNA clamp. *Cell* *69*, 425–437.
- Krishna, T.S., Kong, X.P., Gary, S., Burgers, P.M., and Kuriyan, J. (1994). Crystal structure of the eukaryotic DNA polymerase processivity factor PCNA. *Cell* *79*, 1233–1243.
- Lopez de Saro, F.J., Georgescu, R.E., Goodman, M.F., and O'Donnell, M. (2003). Competitive processivity-clamp usage by DNA polymerases during DNA replication and repair. *EMBO J.* *22*, 6408–6418.
- Lu, X.J., and Olson, W.K. (2003). 3DNA: a software package for the analysis, rebuilding and visualization of three-dimensional nucleic acid structures. *Nucleic Acids Res.* *31*, 5108–5121.
- Matsumiya, S., Ishino, Y., and Morikawa, K. (2001). Crystal structure of an archaeal DNA sliding clamp: proliferating cell nuclear antigen from *Pyrococcus furiosus*. *Protein Sci.* *10*, 17–23.
- Maul, R.W., Scouten Ponticelli, S.K., Duzen, J.M., and Sutton, M.D. (2007). Differential binding of *Escherichia coli* DNA polymerases to the beta-sliding clamp. *Mol. Microbiol.* *65*, 811–827.
- McHenry, C.S. (2003). Chromosomal replicases as asymmetric dimers; studies of subunit arrangement and functional consequences. *Mol. Microbiol.* *49*, 1157–1165.
- McInerney, P., and O'Donnell, M. (2004). Functional uncoupling of twin polymerases: mechanism of polymerase dissociation from a lagging-strand block. *J. Biol. Chem.* *279*, 21543–21551.
- Naktinis, V., Turner, J., and O'Donnell, M. (1996). A molecular switch in a replication machine defined by an internal competition for protein rings. *Cell* *84*, 137–145.
- Otwinowski, Z., and Minor, W. (1997). Processing of the X-ray diffraction data collected in oscillation mode. *Methods Enzymol.* *276*, 307–326.
- Shamoo, Y., and Steitz, T.A. (1999). Building a replisome from interacting pieces: sliding clamp complexed to a peptide from DNA polymerase and a polymerase editing complex. *Cell* *99*, 155–166.
- Snyder, A.K., Williams, C.R., Johnson, A., O'Donnell, M., and Bloom, L.B. (2004). Mechanism of loading the *E. coli* DNA polymerase III sliding clamp: II. Uncoupling the beta and DNA binding activities of the gamma complex. *J. Biol. Chem.* *279*, 4386–4393.
- Stukenberg, P.T., Turner, J., and O'Donnell, M. (1994). An explanation for lagging strand replication: polymerase hopping among DNA sliding clamps. *Cell* *78*, 877–887.
- Sutton, M.D. (2004). The *Escherichia coli* dnaN159 mutant displays altered DNA polymerase Usage and chronic SOS induction. *J. Bacteriol.* *186*, 6738–6748.
- Sutton, M.D., and Walker, G.C. (2001). Managing DNA polymerases: coordinating DNA replication, DNA repair, and DNA recombination. *Proc. Natl. Acad. Sci. USA* *98*, 8342–8349.
- Sutton, M.D., and Duzen, J.M. (2006). Specific amino acid residues in the beta sliding clamp establish a DNA polymerase usage hierarchy in *Escherichia coli*. *DNA Repair (Amst.)* *5*, 312–323.
- Sutton, M.D., Smith, B.T., Godoy, V.G., and Walker, G.C. (2000). The SOS response: recent insights into umuDC-dependent mutagenesis and DNA damage tolerance. *Annu. Rev. Genet.* *34*, 479–497.
- Sutton, M.D., Duzen, J.M., and Maul, R.W. (2005). Mutant forms of the *Escherichia coli* beta sliding clamp that distinguish between its roles in replication and DNA polymerase V-dependent translesion DNA synthesis. *Mol. Microbiol.* *55*, 1751–1766.
- Warbrick, E. (2000). The puzzle of PCNA's many partners. *Bioessays* *22*, 997–1006.
- Yao, N., Hurwitz, J., and O'Donnell, M. (2000). Dynamics of beta and proliferating cell nuclear antigen sliding clamps in traversing DNA secondary structure. *J. Biol. Chem.* *275*, 1421–1432.

#### Accession Numbers

Data describing the structure of the  $\beta$ -DNA (10/14-mer) complex have been deposited in the RCSB Protein Data Bank under PDB code 3BEP.